Figure S1. Gating strategy of PI cell cycle experiments. Gating strategy for cell cycle analysis in Fig. 1D. FSC, forward scatter; SSC, side scatter; PE, phycoerythrin.

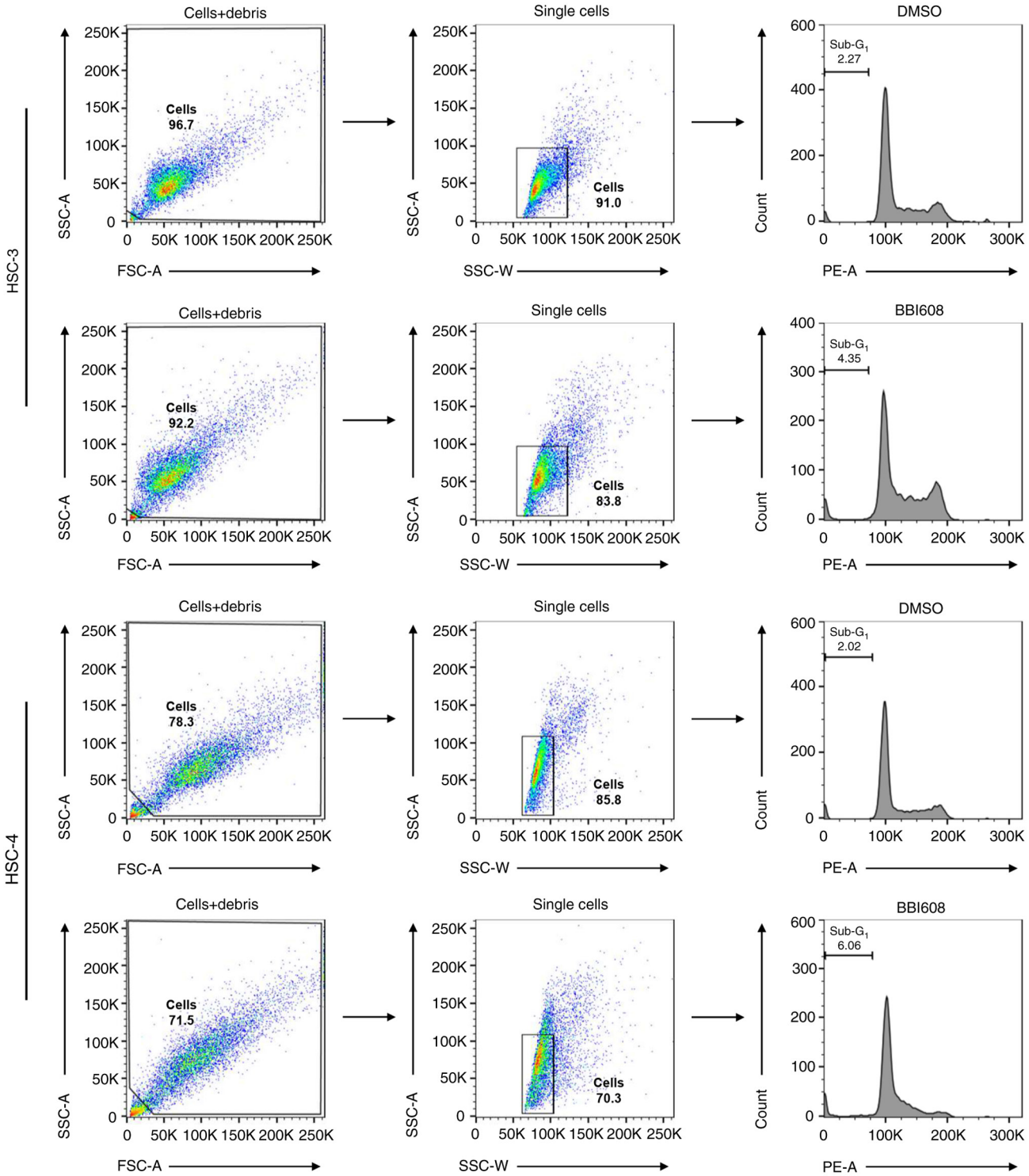

Figure S2. Effect of BBI608 on oral squamous cell carcinoma cell proliferation. Exposure to BBI608 inhibits oral squamous cell carcinoma cell proliferation in a concentration-dependent manner. (A) Representative concentration-response curves from the Cell Counting Kit-8 assay showing the effect of BBI608. (B) Representative images of crystal violet staining illustrating the response to BBI608. All experiments were conducted in triplicate.

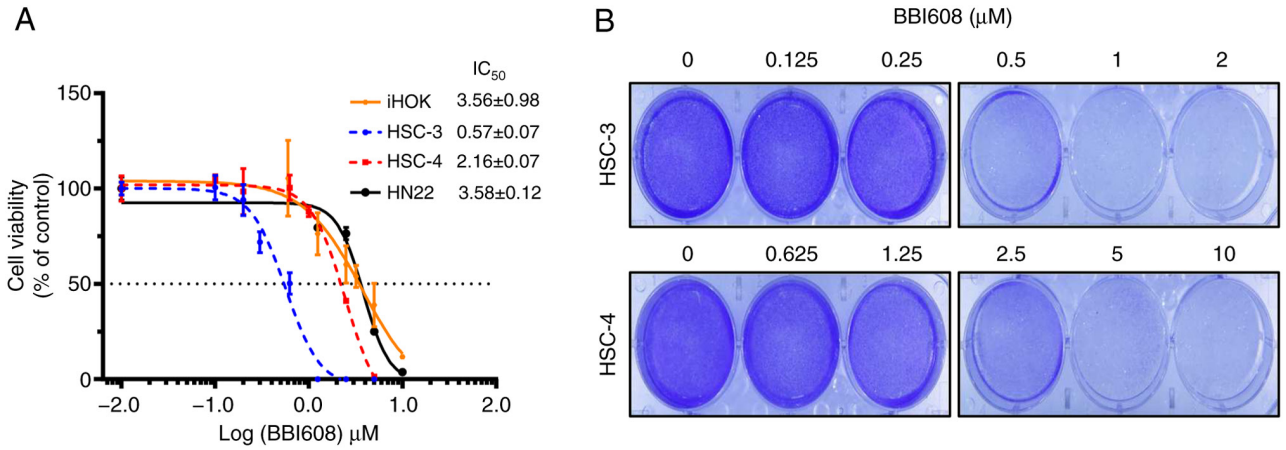

Figure S3. Concentration-dependent effect of BBI608 on cytotoxicity and apoptosis in oral squamous cell carcinoma cells. (A) Cell viability was assessed by trypan blue exclusion assay. (B) Western blot analysis examining the expression of p-STAT3(Y705), c-PARP, total STAT3, total PARP and β-actin (loading control). The expression levels of p-STAT3(Y705) and c-PARP were normalized to those of total STAT3 and PARP, respectively. All experiments were performed in triplicate, and the results are presented as the mean ± SD. *P<0.05 vs. 0 μM. p, phosphorylated; c, cleaved; PARP, poly(ADP-ribose) polymerase.

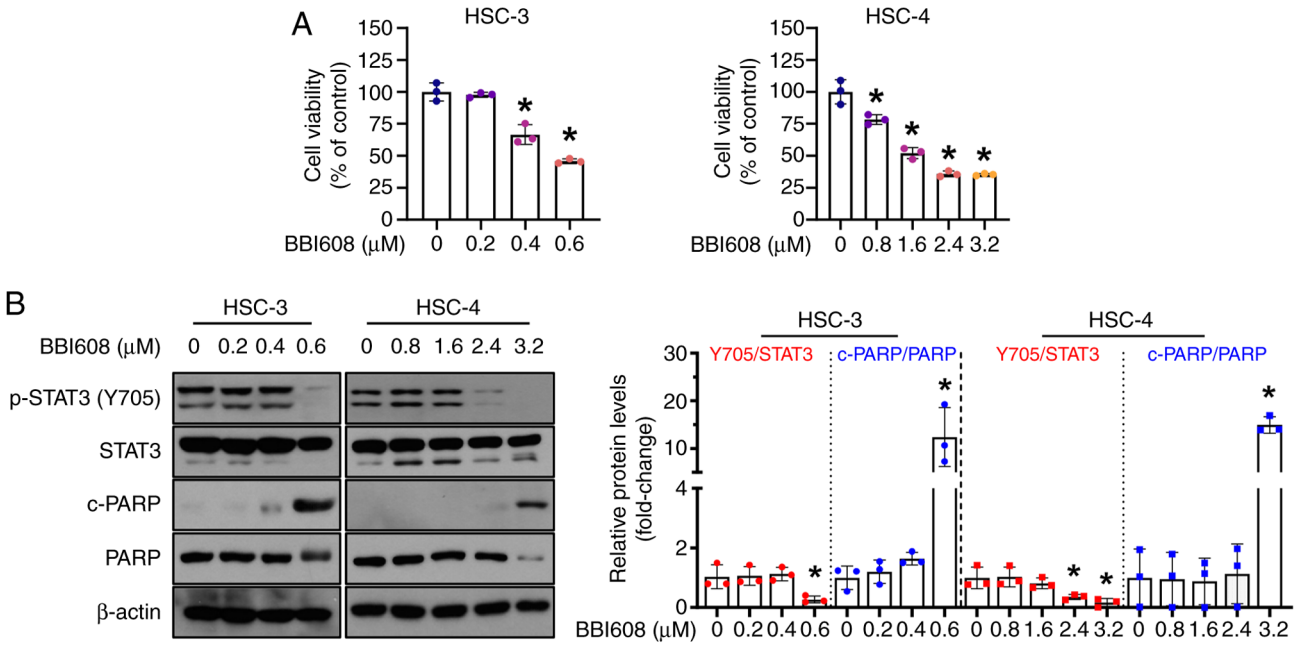

Figure S4. Concentration-dependent inhibitory effect of Z-VAD-FMK on c-PARP induction in oral squamous cell carcinoma cells. Western blot analysis demonstrating the expression levels of c-PARP, total PARP and β-actin (loading control). The expression levels of c-PARP were normalized to those of total PARP. All experiments were conducted in triplicate and the results are presented as the mean ± SD. *P<0.05; #P<0.05. c, cleaved; PARP, poly(ADP-ribose) polymerase.

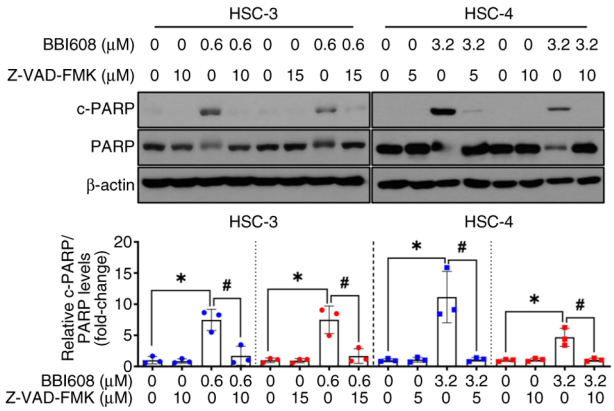

Figure S5. Effects of BBI608 on cell cycle distribution and apoptosis in oral squamous cell carcinoma cells. (A) Cell cycle distribution of HSC-3 and HSC-4 cells treated with DMSO or BB608 at concentrations of 0.4 and 3.2 μM, respectively, for 24 h. (B) Apoptosis analysis was evaluated by Annexin V/PI staining. HSC-3 and HSC-4 cells were pre-treated with Z-VAD-FMK at 10 and 5 μM for 1 h, followed by treatment with BBI608 at 0.6 and 3.2 μM for 24 h, respectively. All experiments were conducted in triplicate and the results are presented as the mean ± SD. *P<0.05; #P<0.05. PE, phycoerythrin.

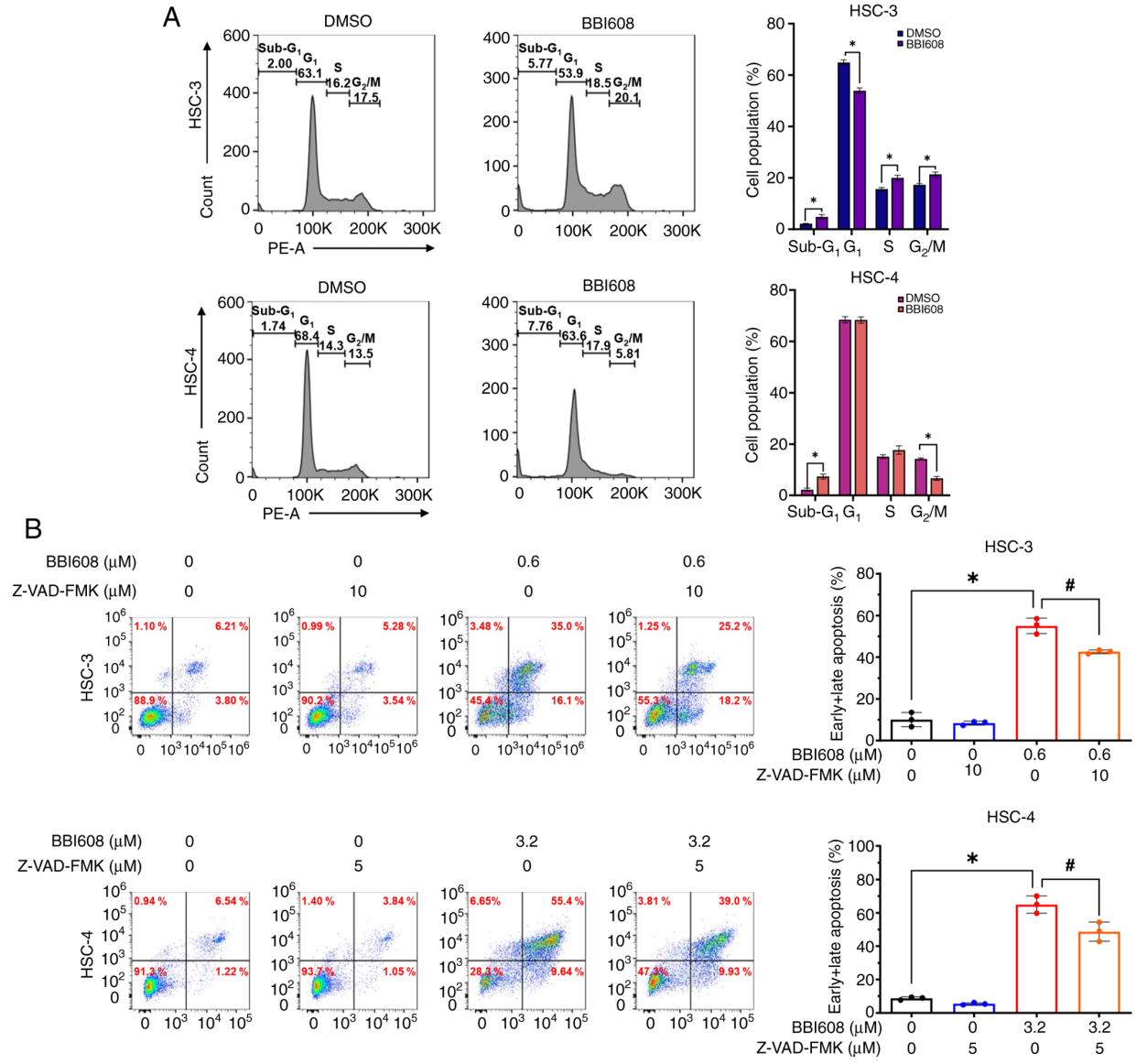

Figure S6. Inhibitory effects of BBI608 on STAT3 signaling related to apoptosis induction in oral squamous cell carcinoma cells. HSC-3 and HSC-4 cells were treated with 0.6 and 3.2 μM BBI608, respectively, at different time points, followed by western blot analysis. Protein expression levels were normalized to those of β-actin, except for p-STAT3 and c-PARP levels, which were normalized to those of total STAT3 and PARP, respectively. All experiments were performed in triplicate, and the results are presented as the mean ± SD. *P<0.05. Mcl-1, myeloid cell leukemia-1; p, phosphorylated; c, cleaved; PARP, poly(ADP-ribose) polymerase.

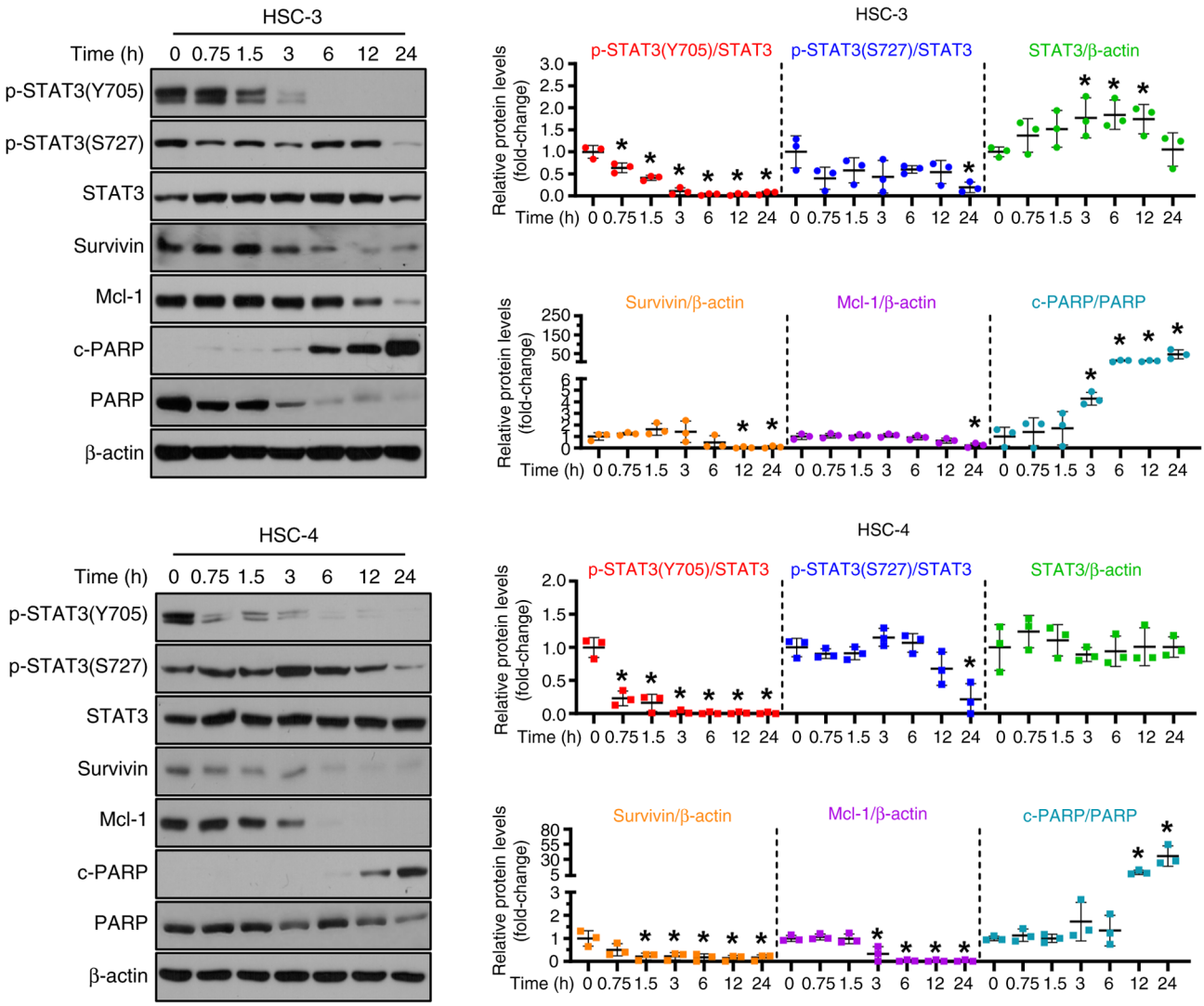

Figure S7. ERK and GSK3β signaling are not involved in the decrease of Mcl-1 stability induced by BBI608 treatment. HSC-3 and HSC-4 cells were treated with 0.6 and 3.2 μM BBI608, respectively at different time points, and western blot analysis was conducted to measure p-Mcl-1, p-GSK3β and p-ERK1/2, as well as total Mcl-1, GSK3β and ERK1/2. β-actin served as an internal control. The expression levels of p-Mcl-1, p-GSK3β and p-ERK1/2 were normalized to those of total Mcl-1, GSK3β and ERK1/2, respectively. All experiments were performed in triplicate, and the results are presented as the mean ± SD. *P<0.05. Mcl-1, myeloid cell leukemia-1; p, phosphorylated.